# The luminescence characterization and structure of $Eu^{2+}$ doped $LiMgPO_4$



2010 J. Phys.: Condens. Matter 22 235402

(http://iopscience.iop.org/0953-8984/22/23/235402)

J. Phys.: Condens. Matter **22** (2010) 235402 (6pp) doi:10.1088/0953-8984/22/23/235402

# The luminescence characterization and structure of $Eu^{2+}$ doped $LiMgPO_4$

**Suyin Zhang[1], Yanlin Huang[1], Liang Shi[2] and Hyo Jin Seo[2,3]**

[1] College of Chemistry, Chemical Engineering and Materials Science, Soochow University, Suzhou 215123, People's Republic of China
[2] Department of Physics, Pukyong National University, Busan 608-737, Republic of Korea

E-mail: hjseo@pknu.ac.kr (H J Seo) and huang@suda.edu.cn (Y Huang)

Received 19 January 2010, in final form 16 March 2010
Published 26 May 2010
Online at stacks.iop.org/JPhysCM/22/235402

**Abstract**
An $Eu^{2+}$-doped $LiMgPO_4$ phosphor was prepared by a high temperature solid-state reaction. The formation was confirmed by x-ray powder diffraction measurements to be a single $LiMgPO_4$ phase. The photoluminescence excitation and emission spectra were investigated. The luminescence shows a broad emission from the $4f^6 5d \rightarrow 4f^7(^8S_{7/2})$ transition at room temperature. At low temperature the zero-phonon line for transitions to the $4f^7$ ($^8S_{7/2}$) level of the $4f^6(^7F_j)5d^1$ excited state is observed at 360 nm and it is found that the emission line of the $4f^7(^6P_{7/2}) \rightarrow 4f^7(^8S_{7/2})$ transition overlaps the zero-phonon line at nearly the same position of 360 nm. The influences of temperature on the luminescence spectra and decay times were investigated. The doping mechanism of $Eu^{2+}$ ions in $LiMgPO_4$ was discussed. The $Eu^{2+}$ ions were suggested to occupy the $Li^+$ sites in $LiMgPO_4$ to induce the small crystal field splitting and weak nephelauxetic effect.

(Some figures in this article are in colour only in the electronic version)

## 1. Introduction

Optical transitions of $Eu^{2+}$ ions have been investigated in many compounds. The luminescence of $Eu^{2+}$ is generally due to parity allowed electric dipole transitions from the lowest band of the $4f^6 5d^1$ configuration to the $^8S_{7/2}$ ground state of the $4f^7$ configuration (hereafter $5d \rightarrow 4f$). The allowed $5d \rightarrow 4f$ electric dipole transitions give rise to broad band emission when the lowest 5d level is below the first excited $4f^7$ state, which is the most common situation [1].

If the influence of the crystal field and nephelauxetic effect are weak, the lowest component of the 5d configuration lies in such a position that the energy is higher than the excited 4f (the excited 4f state is called the $4f'$ state) configuration. At low temperature, it is possible that the excited $Eu^{2+}$ ions relax to the $4f'$ level. Although $4f' \rightarrow 4f$ transition is parity forbidden, sharp line emission spectra due to the $4f^7(^6P_{7/2}) \rightarrow 4f^7(^8S_{7/2})$ also can be observed (hereafter $4f \rightarrow 4f$) [2]. For example, $4f \rightarrow 4f$ transitions of $Eu^{2+}$ ions were observed in $MBe_2Si_2O_7$ (M = Sr, Ba) [3], $LiBaF_3$ [4], $KMgF_3$ [5], $BaY_2F_8$ [6], $MF_2$–$MF_2$–$AlF_3$ (M = Ca, Sr, Ba) [7] and $MSO_4$:(M = Ca, Sr, Ba) [8]. However, to the best of our knowledge, the $4f \rightarrow 4f$ transition of $Eu^{2+}$ has not been reported in a phosphate host.

The phosphate with $ABPO_4$ formula (A and B are mono- and divalent cations, respectively), are a large family of mono-phosphates with different structure types depending on the relative size of the A and B ions [9]. If the size of the A and B are small, such as $Li^+$ and $Mg^{2+}$, the resulting compound $LiMgPO_4$ adopts the olivine ($Mg_2SiO_4$) type structure [10]. Since 1965 these kinds of mono-phosphates, e.g. $LiMPO_4$ (M = Mg, Mn, Co, Ni) have attracted much attention because they have very interesting magnetoelectric properties [11]. The magnetic properties of $LiMgPO_4$ doped with Co or Fe have been widely investigated, which exhibit antiferromagnetic behaviors with some differences in the ordering temperatures [11, 12]. However, the luminescence properties are rarely reported. $LiMgPO_4Mg^{2+}$ and $Li^+$ have six coordinations (CNs) with ionic radii of 0.72 and 0.76 Å, respectively [13, 14]. It seems interesting to study whether it is possible to dope the large $Eu^{2+}$ ion (the ionic radius with CN = 6 is 1.17 Å [13, 14]) into the $LiMgPO_4$ lattice and to present its luminescence properties.

[3] Author to whom any correspondence should be addressed.

 

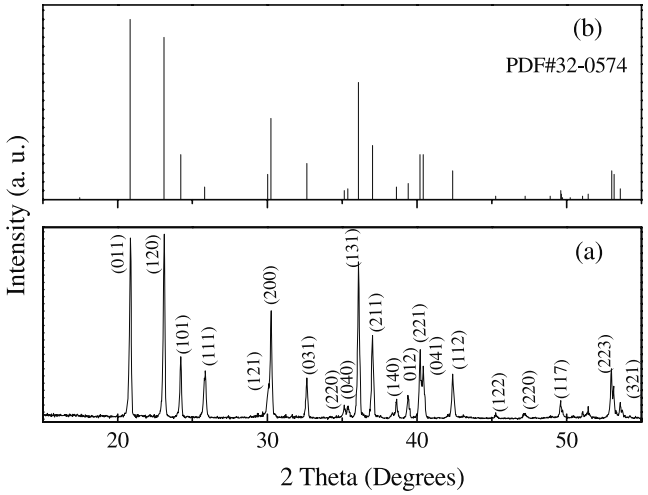


**Figure 1.** XRD pattern of $LiMgPO_4:Eu^{2+}$ in this work (a) and JCPDS card No. 32-0574 (b).

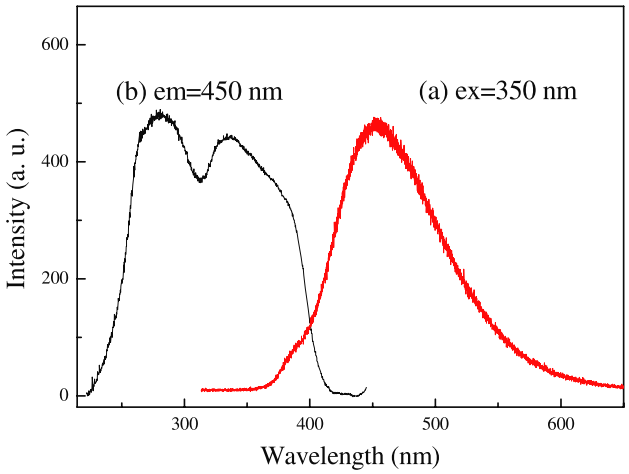


**Figure 2.** The photoluminescence emission (a) and excitation spectra (b) of $LiMgPO_4:Eu^{2+}$ at RT.

In the present work, $Eu^{2+}$-doped $LiMgPO_4$ was synthesized. The emission spectra and decay curves of the $Eu^{2+}$ ions were measured. The zero-phonon line of the lowest $4f^65d^1 \rightarrow 4f^7(^8S_{7/2})$ band at 360 nm overlapped by the emission line of the $4f^7(^6P_{7/2}) \rightarrow 4f^7(^8S_{7/2})$ transition of $Eu^{2+}$ in $LiMgPO_4$ was observed. The lifetime of the parity allowed d–f transition is much shorter than that of the parity forbidden f′–f transition. The doping mechanism of $Eu^{2+}$ in $LiMgPO_4$ is discussed.

## 2. Experimental details

The preparation of $LiMgPO_4:Eu^{2+}$ was carried out by solid-state synthesis. The raw materials were $Li_2CO_3$ (99.9%), $4(MgCO_3)\cdot Mg(OH)_2\cdot 5H_2O$ (magnesium carbonate basic pentahydrate, 99.9%), $NH_4H_2PO_4$ (99.9%) and $Eu_2O_3$ (99.9%). The doping level of $Eu^{2+}$ is 1.0 mol% of $Li^+$. The starting materials with stoichiometric amounts were ground together in an agate mortar. The mixture was firstly heated up to 300 °C and kept at this temperature for 5 h. After a second homogenization in the mortar in acetone, the sample was heated up to 650 °C and kept at this temperature for 10 h in air. After that, the sample was mixed and heated at 800 °C for 20 h in a crucible along with the reducing agent (active carbon). The products were quenched to room temperature.

The photoluminescence spectra were recorded on a Perkin-Elmer LS-50B luminescence spectrometer with Monk–Gillieson type monochromators and a xenon discharge lamp as excitation source. The spectroscopic measurements at low temperature were performed by a pulsed Nd:YAG laser at 266 nm (Spectron Laser System SL802G). The samples were attached to a holder which was placed in a helium gas flow cryostat in a variable temperature region (10–300 K). The lifetimes were measured for $LiMgPO_4:Eu^{2+}$. The luminescence was dispersed by the 75 cm monochromator (Acton Research Corp. Pro-750) and multiplied by a photomultiplier tube (PMT) (Hamamatsu R928). The data were displayed and recorded with a LeCloy 9301 digital storage oscilloscope.

## 3. Results and discussion

### *3.1. Phase formation*

The x-ray powder diffraction (XRD) pattern of $LiMgPO_4:Eu^{2+}$ together with the Joint Committee on Powder Diffraction Standards details (JCPDS No. 50-0146) are shown in figure 1. By a comparison between them, the position and intensity of the peaks are the same. No impurity lines were observed and all the reflections could be well indexed to a $LiMgPO_4$ single phase. The lattice parameters analyzed using the Jade-5.0 software program are $a = 10.148$ Å, $b = 5.910$ Å, $c = 4.694$ Å, $V = 281.521$ Å$^3$. These results agree well with the reported data of pure $LiMgPO_4$, i.e. $a = 10.147$ Å, $b = 5.909$ Å, $c = 4.692$ Å, $V = 281.326$ Å$^3$ [10]. This suggests that the $Eu^{2+}$ ions are incorporated into the lattice. When there are $Eu^{2+}$ ions doped in the structure, the cell lattice will expand, since the radii of $Eu^{2+}$ ions (CN = 6, 1.17 Å) are larger than the radii of $Li^+$ (CN = 6, 0.76 Å) and $Mg^{2+}$ (CN = 6, 0.72 Å) ions [13, 14]. Consequentially, the average lattice and volume of a unit cell of $LiMgPO_4$ increase with $Eu^{2+}$ doping content.

### *3.2. Photoluminescence and assignment of $Eu^{2+}$ emission*

The room temperature (RT) excitation and emission spectra of $LiMgPO_4:Eu^{2+}$ are shown in figure 2. Under an excitation of 350 nm, the emission spectra consist of a broad band from 370 to 600 nm with a maximum wavelength at 450 nm, which can be ascribed to the 5d → 4f allowed transition of $Eu^{2+}$ ions (figure 2(a)). The excitation spectrum (figure 2(b)) shows that $LiMgPO_4:Eu^{2+}$ has two broad absorption bands, namely the band that extends from about 220 to 313 nm and the other band between about 320 and 400 nm, which can be attributed to the splitting of the $4f^65d^1$ electronic configuration into the lower state $4f^65d^1$ (e) and the higher state $4f^65d^1$ (t) of $Eu^{2+}$ [1, 2].

The Stokes' shift of the $Eu^{2+}$ emission is defined as the difference between the absorption energy of the $4f^7[^8S_{7/2}] \rightarrow 4f^6[^7F_0]5d^1$ transition and the emission energy [15]. It is

**Table 1.** The lifetime values of 5d → 4f transitions at different temperatures.

| Temperature (K) | 10 | 50 | 75 | 100 | 150 | 200 | 230 | 250 | 270 | 300 |
|---|---|---|---|---|---|---|---|---|---|---|
| $\tau_{380\ nm}$ ($\mu$s) | 0.243 | 0.238 | 0.227 | 0.215 | 0.208 | 0.191 | 0.182 | 0.161 | 0.155 | 0.154 |
| $\tau_{450\ nm}$ ($\mu$s) | 0.387 | 0.381 | 0.375 | 0.361 | 0.355 | 0.336 | 0.295 | 0.226 | 0.201 | 0.189 |

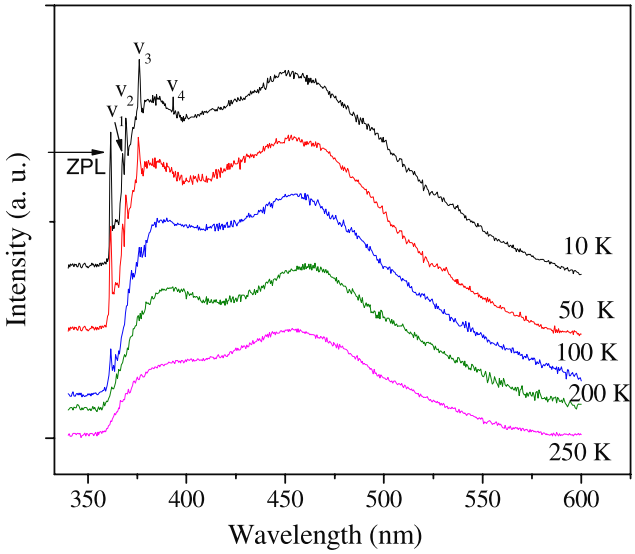


**Figure 3.** The emission spectra of $LiMgPO_4$:$Eu^{2+}$ at 266 nm laser excitation. Line emissions peaking at 360 nm are due to the 4f → 4f transitions. The broad band emissions are due to the 5d → 4f transitions. The other sharp peaks are due to Stokes' vibrations.

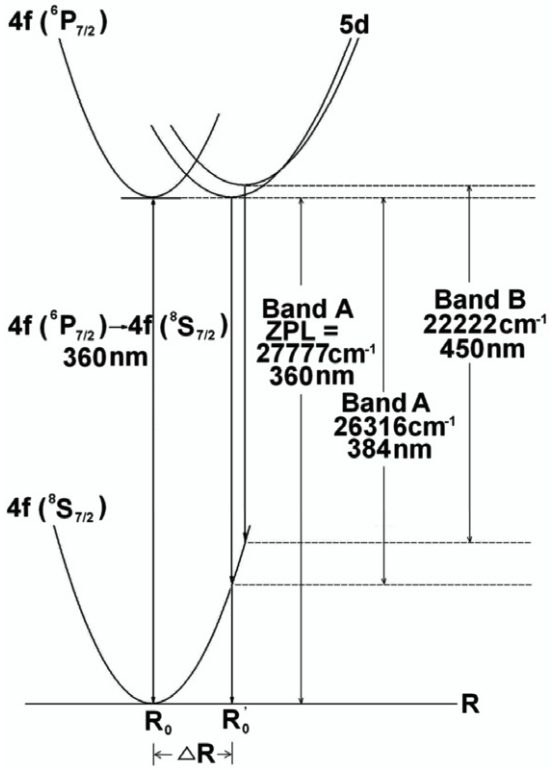


**Figure 4.** The configurational coordinate diagram model of the $Eu^{2+}$ ion in the $LiMgPO_4$. EXC is the excitation process. EM is the emission process. There is an offset ($\Delta R$) between the parabolas of the ground and excited states.

common practice to determine it by the energy difference between the maximum of the lowest excitation band (350 nm, 28 570 $cm^{-1}$) and that of the emission band (450 nm, 22 222 $cm^{-1}$). The Stokes' shift in $LiMgPO_4$:$Eu^{2+}$ was calculated to be 6, 348 $cm^{-1}$.

The emission spectra were obtained at low temperature and are shown in figure 3. The two broad emission bands peaking at 385 and 450 nm due to the $4f^65d^1 \rightarrow 4f^7(^8S_{7/2})$ transitions of $Eu^{2+}$ are observed together with several sharp emission lines between 355 and 400 nm. The emission line at 360 nm is a typical zero-phonon line from the $4f^65d^1$ state to the ground $4f^7(^8S_{7/2})$ state. The sharp lines are quenched above 100 K.

The energy of zero-phonon line, which is defined as the energy between the bottom of the excited $4f^65d^1$ state and the lowest $4f^7(^8S_{7/2})$ state (see figure 4), depends strongly on the crystal field strength acting on $Eu^{2+}$ by surrounding ligands. It is interesting to note that the emission line due to the $4f^7(^6P_{7/2}) \rightarrow 4f^7(^8S_{7/2})$ transition is located at around 360 nm which is nearly independent of the host because the 4f electrons are shielded by the $5s^25p^6$ electron clouds from the crystal field of the host. For example, it has been reported to be 360 nm in $MSO_4$ (M = Mg, Sr, Ba) [8], 358 nm in $\alpha$-$BaAlF_5$, $\beta$-$BaAlF_5$ and $Ba_3Al_2F_{12}$ [7], 358 nm in $BaY_2F_8$ [6], 360 nm in $SrAl_{12}O_{19}$ and $BaAl_{12}O_{19}$ [3], 360 nm in $LiBaF_3$ [4] and 358 nm in $K_2MgF_4$ [16].

To confirm the origin of the emission line at around 360 nm the decay curves were measured for the sharp emission line and the broad emission bands as shown in figure 5. It is surprising to observe the much longer decay time (850 $\mu$s at 10 K) of the line emission at 360 nm than the decay times of 0.243 and 0.387 $\mu$s of the broad emission bands at 380 and 450 nm, respectively. If the line at 360 nm originates from the zero-phonon line of the 5d–4f transition the decay time should be the same as that of the broad band. Thus we attribute the line at 360 nm to originate from the forbidden $4f^7(^6P_{7/2}) \rightarrow 4f^7(^8S_{7/2})$ transition, which is overlapped with the zero-phonon line of the 5d–4f transition [1]. The different decay times between the bands at 380 and 450 nm imply that there exist two different substitution sites for $Eu^{2+}$ in the $LiMgPO_4$ lattice. The non-exponential decay curves observed for the 5d–4f transition in figure 5(a) may be caused by some energy transfer and the possible multisite structure of $Eu^{2+}$ ions.

The decay times are listed in table 1. From 10 to 300 K the lifetimes of the 380 nm and 450 nm emissions decrease from 0.243 to 0.154 $\mu$s and 0.387 to 0.189 $\mu$s, respectively. The decay of the 360 nm emission shows single-exponential decay and the decay time shortens from 850 to 470 $\mu$s with increasing

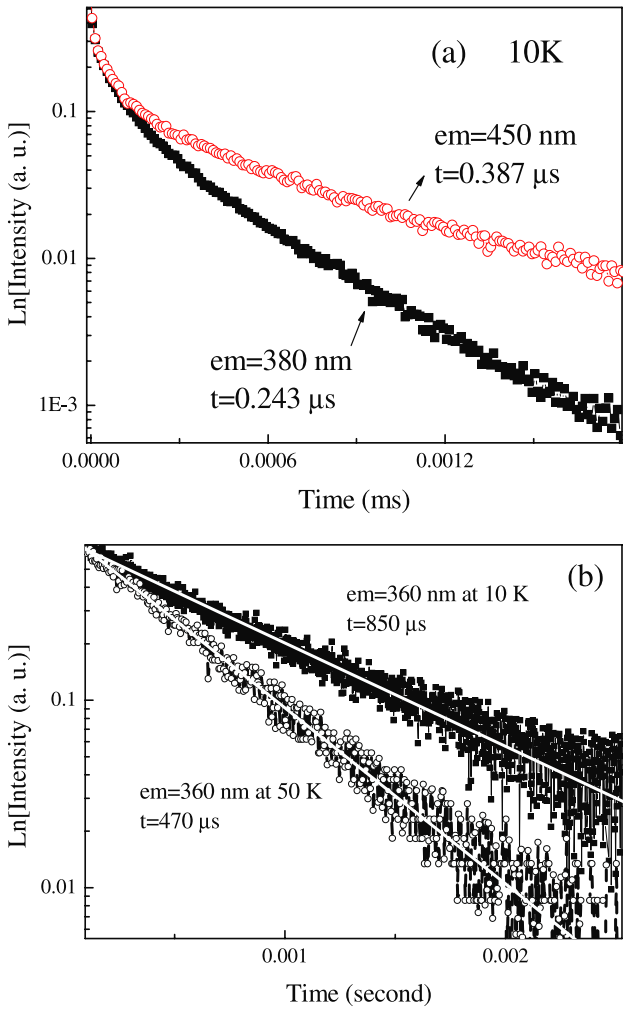


**Figure 5.** The luminescence decay curves of 5d → 4f transitions at 10 K (a) and the 4f → 4f transitions at 10 and 50 K (b).

temperature from 10 and 50 K. The other sharp lines at 367.2, 369.2, 376 and 393.2 nm at low energy sites are due to the vibrational progressions which will be discussed elsewhere.

### *3.3. The doping mechanism of $Eu^{2+}$ in $LiMgPO_4$*

To the best of our knowledge, this is the first time the 4f → 4f transition of an $Eu^{2+}$ ion in a phosphate host has been reported. Why does the line emission of the $Eu^{2+}$ ion occur in the $LiMgPO_4$ host? A required condition is that the lowest 5d level of the $Eu^{2+}$ ion is above or at a similar level to the lowest excited 4f($^6P_{7/2}$) level. Usually, the positions of the 5d level of $Eu^{2+}$ are strongly influenced by the host lattices, while the 4f levels have nearly fixed positions [1]. To answer this question, the crystal structure of $LiMgPO_4$ and the doping mechanism of $Eu^{2+}$ in this host should be elucidated. Note that in $LiMgPO_4$ there are two sites for the possible substitution of $Eu^{2+}$, i.e. $Li^+$ and $Mg^{2+}$.

$LiMgPO_4$ is orthorhombic, with the space group *Pnma* with *a* about twice the *b* and *c* cell constants [11]. Figure 6 shows a schematic view of the $LiMgPO_4$ structure. The structure contains tetrahedral $PO_4$ and octahedral $LiO_6$ and

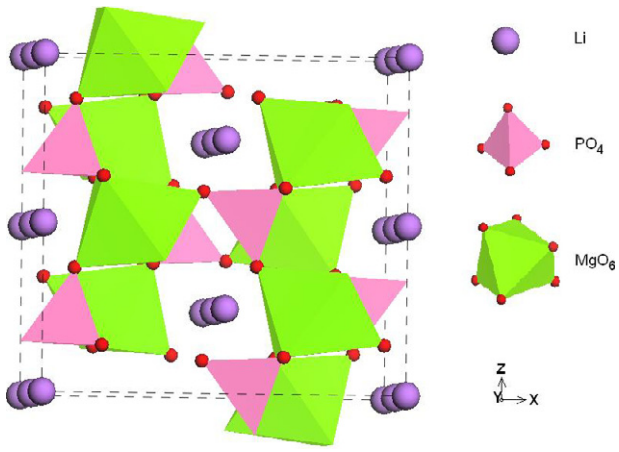


**Figure 6.** A schematic view of the $LiMgPO_4$ structure.

$MgO_6$ groups. It belongs to the ordered olivine-type structure. This structure can be seen as a hexagonal close packing of oxygens with the $Li^+$ and $Mg^{2+}$ located in the center of octahedral sites, and the P in the 1/8 of tetrahedral sites. The $MgO_6$ distorted octahedra are corner shared and cross-linked by the $PO_4$ groups, forming a three-dimensional network, with perpendicular tunnels along the [010] and [001] directions [10]. The tunnels are occupied by Li ions as can be seen in figure 6.

In the $LiMgPO_4$ $Li^+$ ion (CN = 6) has an ionic radius of 0.76 Å, while $Mg^{2+}$ (CN = 6) has an ionic radius of 0.72 Å [13, 14]. Both ions have a large difference when compared to $Eu^{2+}$, which has an ionic radius of 1.17 Å [13, 14]. However, taking into account the structural description, there is considerable preference for the substitution of $Li^+$ ions, as the $Li^+$ ions occupy the structural tunnels in the three-dimensional network forming strips running zig-zag along *b* (figure 6). The average bond distances Li–O and Mg–O are 2.143 and 2.105 Å within polyhedra $LiO_6$ and $MgO_6$, respectively. The average O–O edge lengths in polyhedra $LiO_6$ and $MgO_6$ are 3.015 and 2.921 Å, respectively [10].

In spite of a considerable difference between the ionic radii of $Li^+$ and the divalent $Eu^{2+}$, it is reasonable that the $Eu^{2+}$ ions may probably occupy the $Li^+$ sites because the compact space of the $Mg^{2+}$ ions with short Mg–O distance in $LiMgPO_4$ offers too small a site for the $Eu^{2+}$ ions. A big rare earth ion substituting $Li^+$ ions is possible in a crystal. For example, the substitutions of $Li^+$ by $Eu^{3+}$ in $LiNbO_3$ [17] and $LiTaO_3$ [18] have been reported.

In $Eu^{2+}$-doped $LiMgPO_4$, the substitution of the $Li^+$ site by the $Eu^{2+}$ results in a positive charge $(Eu^{2+}_{Li})^{\bullet}$. The replacement requires charge compensation. In general, the required charge compensation can be achieved by two possible mechanisms: firstly, $Eu^{2+}$ ions substitute for $Li^+$ and combine with an $Li^+$ vacancy: $Li^+ \rightarrow Eu^{2+} + V'_{Li}$ forming the dipole complexes of $[(Eu^{2+}_{Li})^{\bullet}–V'_{Li}]$. Such a charge compensation mechanism is very common. Secondly, another charge compensation mechanism related to the interstitial oxygen $O''_i$ is possible: $2Li^+ \rightarrow 2Eu^{2+} + O''_i$. This mechanism could form the dipole complexes of $[2(Eu^{2+}_{Li})^{\bullet}–O''_i]$. Usually, in the oxide

components, the reaction energy to create the $O_i''$ is higher than that of the cation vacancy [19]. This defect ($O_i''$) tends to increase the CN of the $Eu^{2+}$ ion, resulting in an increase of its atomic radius [18]. This is unfavorable for the substitution of $Li^+$.

It could be suggested that the substitution of an $Li^+$ ion by an $Eu^{2+}$ can be represented by the incorporation of $V'_{Li}$. This kind of mechanism was also confirmed in $Fe^{3+}$ doped $LiMgPO_4$, where $Fe^{3+}$ substitutes the $Li^+$ ions in the channels of the $LiMgPO_4$ structure along the [010] direction, creating cation vacancies $V'_{Li}$ [12]. However, even when the $Li^+$ ions left vacancies in the structure, ionic mobility in $LiMgPO_4$ was not observed. It was suggested that the $Fe^{3+}$ substitution for $Li^+$ pushes the $Li^+$ neighbors into the channels, leaving vacancies as nearest neighbors of the iron. The structure of $Li_{1-x}Fe_xMgPO_4$ is modified with the degree of iron substitution, $x$. The Li(Fe)–O distances undergo a progressive enlargement with the increase of $x$. The Mg–O distances diminish with increasing $x$ and the range of values for the O–Mg–O angles is shorter. Consequently, the $MgO_6$ octahedra become more regular and smaller. Coulomb repulsion between the negatively charged ions will avoid any jumps back to the vacant sites [11].

Supposing this mechanism is working in $LiMgPO_4:Eu^{2+}$, the nature of the emission of $LiMgPO_4:Eu^{2+}$ can be deduced from the crystal structure. Usually, a 4f → 4f transition of an $Eu^{2+}$ ion requires a weak nephelauxetic effect and a weak crystal field in a crystal [20]. For example, a fluorite ligand induces a small nephelauxetic effect so that fluorites are particularly likely to give rise to a 4f → 4f $Eu^{2+}$ emission. $Eu^{2+}$ substitutes the $Li^+$ ion in the channels of the $LiMgPO_4$ structure along the [010] direction, creating cation vacancies $V_{Li}$. The strong Coulomb repulsion between the negatively charged ions will weaken the nephelauxetic effect and push the 5d levels to higher energy. This enhances the barycentric energy position of the 5d level compared to the free ion. Consequentially, at low temperature emission transition from the lowest excited state $^6P_{7/2}$ to the $4f^7(^8S_{7/2})$ ground state can be observed.

Under the excitation of the 266 nm Nd:YAG laser, the $Eu^{2+}$ ion in the $LiMgPO_4$ can be excited to a high energy level directly. Then, the excited $Eu^{2+}$ ions relax to the lowest level of the 5d state. At low temperature the broad 5d → 4f emission band at 450 nm (22 222 $cm^{-1}$ in figure 4) and 384 nm (26 316 $cm^{-1}$ in figure 4) occur and the excited $Eu^{2+}$ ions return to the bottom of the ground state. However, there is another way back to the 4f ground state. The excited $Eu^{2+}$ ions relax to the cross point of the excited 4f and 5d state along the 5d curve. It is possible that the excited $Eu^{2+}$ ions continue to relax to the lowest vibration level of the excited 4f state from this point. Thus, the line emission at 360 nm (27 777 $cm^{-1}$ in figure 4) from the 4f′ state to the ground state occurs. The process is shown in figure 4. However, with increasing temperature, the $^6P_{7/2}$ could mix with the higher 5d states because of the thermal population, only the broad emission transition from 5d to the $4f^7(^8S_{7/2})$ is observed.

As can be seen in figure 3, the emission spectra show the strongest emission around 450 nm and a weak shoulder in the high energy region at 380 nm. The emission spectrum of $LiMgPO_4:Eu^{2+}$ presents an obvious asymmetric profile. This indicates that the $Eu^{2+}$ ions have more than one emission center in the $LiMgPO_4$ lattices. The decay times for both bands are quite different, as shown in figure 5. The doping of $Eu^{2+}$ as the impurities in $LiMgPO_4$ can create different charge-compensated sites. However, this multisite structure will be investigated by the optical properties of the $Eu^{3+}$ ion as a structure probe in the $LiMgPO_4$ lattices.

## 4. Conclusions

$LiMgPO_4:Eu^{2+}$ was prepared by the solid-state reaction. This phosphor shows a pure phase of $LiMgPO_4$. The excitation spectrum shows a very broad band extending from 230 to 400 nm. The luminescence spectrum at 300 K consists of a single band peaked at 450 nm. It has been found that the emission spectrum consists of a broad band and a sharp line located at 360 nm at low temperature. The sharp line at 360 nm originates from the $^6P_{7/2} \rightarrow {}^8S_{7/2}$ transition in the $4f^7$ electronic configuration overlapped with the zero-phonon line of the 5d–4f transition of $Eu^{2+}$ whereas the broad band is related to the $4f^65d \rightarrow 4f^7(^8S^{7/2})$ transition. Above 100 K only the 5d → 4f band emission could be detected on the spectra. The luminescence of the 4f–4f transition shows the typical long decay times of 850 $\mu$s and 470 $\mu$s at 10 and 50 K, respectively. $Eu^{2+}$ substitutes the $Li^+$ in the channels of the $LiMgPO_4$ structure along the [010] direction, creating cation vacancies $V'_{Li}$. The lowest $4f^65d$ level is at high energy for $Eu^{2+}$ in $LiMgPO_4$ due to the small crystal field splitting and weak nephelauxetic effect.

## Acknowledgments

This work was financially supported by a Korea Science and Engineering Foundation (KOSEF) grant funded by the Korean government (Ministry of Education, Science and Technology, MEST, No. 2009-0078682).

## References

[1] Dorenbos P 2003 *J. Lumin.* **104** 239–60
[2] Alcala R, Sardar D K and Sibley W A 1982 *J. Lumin.* **27** 273–84
[3] Verstegen J M P J and Sommerdijk J L 1974 *J. Lumin.* **9** 297–301
[4] Mahlik S, Grinberg M, Shi L and Seo H J 2009 *J. Phys.: Condens. Matter* **21** 235603–10
[5] Su H, Jia Z, Shi C, Xin J and Reid S A 2001 *Chem. Phys. Lett.* **335** 17–22
[6] Latourrette B, Guillen F and Fouassier C 1979 *Mater. Res. Bull.* **14** 865–8
[7] Hoffman Mary V 1972 *J. Electrochem. Soc.* **119** 905–9
[8] Yamashita N, Yamamoto I, Ninagawa K, Wada T, Yamashita Y and Nakao Y 1985 *Japan. J. Appl. Phys.* **24** 1174–80
[9] Amara M B, Vlasse M, Flem G L and Hagenmuller P 1983 *Acta Crystallogr.* C **39** 1483–5

[10] Hanic F, Handlovic M, Burdova K and Majling J 1982 *J. Crystallogr. Spectrosc. Res.* **12** 99–127
[11] Goňi A, Bonagamba T J, Silva M A, Panepucci H, Rojo T and Barberisa G E 1998 *J. Appl. Phys.* **84** 416–21
[12] Goňi A, Lezama L, Pujana A, Arriortua M I and Rojo T 2001 *Int. J. Inorg. Mater.* **3** 937–42
[13] Shannon R D and Prewitt C T 1969 *Acta Crystallogr.* B **25** 925–46
[14] Shannon R D 1976 *Acta Crystallogr.* A **32** 751–67
[15] Meijerink A and Blasse G 1989 *J. Lumin.* **43** 283–9
[16] Belsare D, Joshi C P, Moharil S V, Kondawar V K, Muthal P L and Dhopte S M 2008 *J. Alloys Compounds* **450** 468–72
[17] Muñoz Santiuste J E, Macalik B and García Solé J 1993 *Phys. Rev.* B **47** 88–94
[18] Gasparotto G, Cebim M A, Goes M S, Lima S A M, Davolos M R, Varela J A, Aiva-Santos C O P and Zaghete M A 2009 *J. Appl. Phys.* **106** 063509–13
[19] Lin Q and Feng X 2003 *J. Phys.: Condens. Matter* **15** 1963–73
[20] Flem G L, Parent C and Fouassier C 1983 *J. Less-Commun. Met.* **93** 383–8